

MODELLING AND SIMULATION OF A CONTINUOUS FLUIDIZED-BED DRYER

F. S. LAI[†] and YIMING CHEN

U.S. Grain Marketing Research Laboratory, College Avenue, Manhattan, KS 66506, U.S.A.

and

L. T. FAN

Department of Chemical Engineering, Kansas State University, Manhattan, KS 66506, U.S.A.

(Received 28 May 1985)

Abstract—A fairly rigorous mechanistic model of a continuous fluidized-bed dryer has been developed. It depicts the dynamic interactions between gaseous and solid phases in detail. The performance of the dryer has been simulated numerically based on the model. The effects of the operating parameters on the performance characteristics of the dryer have been investigated. These parameters include the superficial gas velocity, the inlet temperature of the drying gas, the mean residence time of solids and the dryer-wall temperature. The results of simulation based on the present model are compared with those based on an existing model. This comparison shows that the former is a substantial improvement over the latter.

INTRODUCTION

The fluidized-bed dryer possesses many significant features over the conventional packed-bed or moving-bed dryer [see, for example, Váncék *et al.* (1966), Nonhebel and Moss (1971)]. These include the following: (i) drying gas is locally mixed intensively during its passage through the bed; consequently the rate of mass and heat transfer between the gas and solids are high; (ii) the extremely rapid heat transfer enables a relatively high inlet gas temperature to be used; (iii) the time of drying is relatively short.

Because of its numerous advantages, fluidized-bed drying has been increasingly applied in diverse industries in either the batch or continuous mode (Vaněček *et al.*, 1966; Viswanathan *et al.*, 1982). In fact, several papers have been published on the subject of continuous fluidized-bed drying since the late 1950s. A comprehensive account of these and other related publications is available (Viswanathan *et al.*, 1982).

Conventional design procedures for a continuous fluidized-bed dryer have been developed mainly under the assumptions that the bed temperature is uniform, the outlet streams are in thermal or concentration equilibrium, and that fluid mechanistic behaviour of the drying gas is homogeneous; in other words, the drying gas is not partitioned into different phases of the fluidized bed, such as the emulsion and bubble phases [see, for example, Nonhebel and Moss (1971), Palancz and Parti (1973)]. Although these assumptions are valid in some circumstances, they may not hold under certain actual situations. The aim of this work is to develop a fairly rigorous and comprehensive mechanistic model without imposing such assumptions. The model can predict the temperature and

moisture content of the outlet gas and also the average moisture content and temperature of the solids at the exit. It will be amply demonstrated that the proposed model represents a significant improvement over an existing mechanistic model for the continuous fluidized-bed dryer proposed by Palancz (1983).

MATHEMATICAL MODELLING

A schematic diagram of the model is shown in Fig. 1. The present model is based on the two-phase theory of fluidization (see, for example, Davidson and Harrison, 1963). The underlying assumptions of this theory are

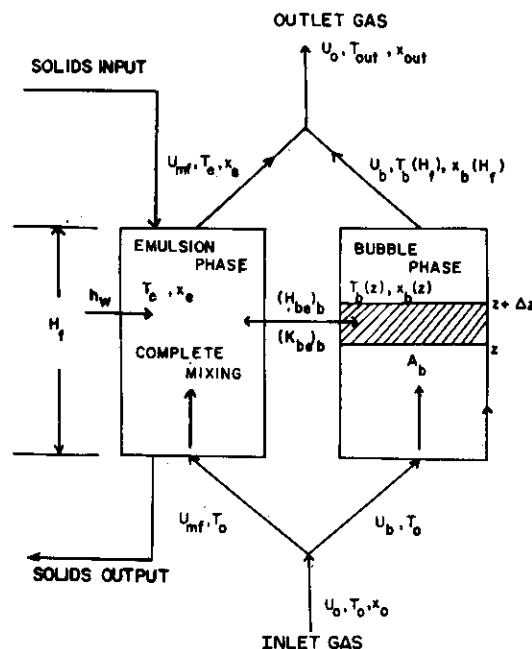


Fig. 1. Schematic diagram of continuous drying in the fluidized bed.

[†]To whom correspondence should be addressed.

that the bed is divided into two phases, a bubble phase and an emulsion phase (which remains in minimum fluidization conditions), and that the excess flow of the fluidizing fluid above minimum fluidization conditions passes through the bed as bubbles. The fluid in the bubble and emulsion phases and the solid particles are considered to be continua. Additional simplifying assumptions imposed in deriving the present model are as follows:

- (1) The bubble phase is solid-free and the size of the bubbles is uniform and fixed at the so-called effective bubble size.
- (2) The movement of bubbles through the bed is of plug flow.
- (3) The clouds surrounding the rising bubbles are very thin and, therefore, the bubble phase exchanges mass and energy only with the emulsion gas.
- (4) The emulsion gas and solid particles are perfectly mixed.
- (5) Solid particles are added and removed at a constant rate.
- (6) The inlet temperature and moisture content of solids are assumed to be uniform.
- (7) The internal resistance of solids to mass and heat transfer is negligible.
- (8) Particles are considered to be uniform in size, shape and physical properties.
- (9) The temperature and moisture content of each particle depend on its age, t_s , that is, the length of its stay in the dryer. As a consequence of assumptions (4) and (5), the residence time distribution function for solids under a steady-state condition is

$$f(t_s) = \frac{1}{t_s} \exp\left(-\frac{t_s}{t_s}\right) \quad (1)$$
- (10) Viscous dissipation is negligible.
- (11) The changes in the physical properties of both solids and drying gas due to the change of temperature are negligible.

These assumptions give rise to the mass and energy conservation equations for each phase of the fluidized-bed dryer.

Mass conservation equations

(A) *Bubble phase.* A steady-state moisture balance around the controlled volume depicted in Fig. 1 gives

$$\frac{U_b}{\delta_b} \frac{dx_b}{dz} = (K_{be})_b (x_e - x_b) \quad (2a)$$

with the boundary condition

$$x_b = x_0 \quad \text{at} \quad z = 0. \quad (2b)$$

Integration of eq. (2a), subject to eq. (2b), gives

$$x_b = x_e - (x_e - x_0) \exp\left[\frac{-(K_{be})_b \delta_b}{U_b} z\right]. \quad (3)$$

The parameters in this expression are evaluated from the following relationships:

1. The bed fraction of the bubble phase, δ_b :

$$\delta_b = 1 - \frac{H_{mf}}{H_f} \quad (4)$$

where H_f/H_{mf} is given by (Babu *et al.*, 1978)

$$\frac{H_f}{H_{mf}} = 1 + \frac{14.311(U_0 - U_{mf})^{0.738} d_p^{1.006} \rho_p^{0.736}}{U_{mf}^{0.937} \rho_g^{0.126}} \quad (5)$$

Alternatively,

$$\delta_b = \frac{(U_0 - U_{mf})}{(U_0 - U_{mf}) + U_{br}} \quad (6)$$

where U_{br} is given by (Davison and Harrison, 1963)

$$U_{br} = 0.711(gd_b)^{0.5} \quad (7)$$

2. The superficial gas velocity through the bubble phase, U_b :

$$U_b = U_0 - U_{mf} \quad (8)$$

3. The minimum fluidization velocity, U_{mf} (Wen and Yu, 1966):

$$\frac{d_p U_{mf} \rho_g}{\mu_g} = \left((33.7)^2 + 0.0408 \frac{d_p^3 \rho_g (\rho_{ws} - \rho_g) g}{\mu_g^2} \right)^{0.5} - 33.7 \quad (9)$$

4. The gas interchange coefficient based on the volume of bubbles, $(K_{be})_b$ (Kunii and Levenspiel, 1969):

$$(K_{be})_b = \frac{1}{1/(K_{ce})_b + 1/(K_{bc})_b} \quad (10)$$

where

$$(K_{bc})_b = 4.5 \frac{U_{mf}}{d_b} + 5.85 \frac{D_g^{1/2} g^{1/4}}{d_b^{5/4}} \quad (11)$$

$$(K_{ce})_b = 6.78 \left(\frac{\varepsilon_{mf} D_{eff} U_b}{d_b^3 \delta_b} \right)^{1/2} \quad (12)$$

with

$$D_{eff} = \varepsilon_{mf} D_g \quad (13)$$

ε_{mf} in the above expression can be approximated by (Broadhurst and Becker, 1975)

$$\varepsilon_{mf} = 0.586 \phi_s^{-0.72} \left[\frac{\mu_g^2}{\rho_g (\rho_{ws} - \rho_g) g d_p^3} \right]^{0.029} \left(\frac{\rho_g}{\rho_{ws}} \right)^{0.021} \quad (14)$$

(B) *Emulsion gas.* From a moisture balance around the entire emulsion gas, illustrated in Fig. 2, we obtain

$$0 = (U_{mf} A_t) \rho_g (x_0 - x_e) + \int_0^{H_f} A_b \rho_g (K_{be})_b (x_b - x_e) dz + (H_f A_t) (1 - \delta_b) (1 - \varepsilon_{mf}) \left(\frac{6}{d_p} \right) \sigma (\bar{x}_p^* - x_e). \quad (15)$$

If we define the average moisture content of gas bubbles, \bar{x}_b , as

$$\bar{x}_b = \frac{1}{H_f} \int_0^{H_f} x_b dz, \quad (16)$$

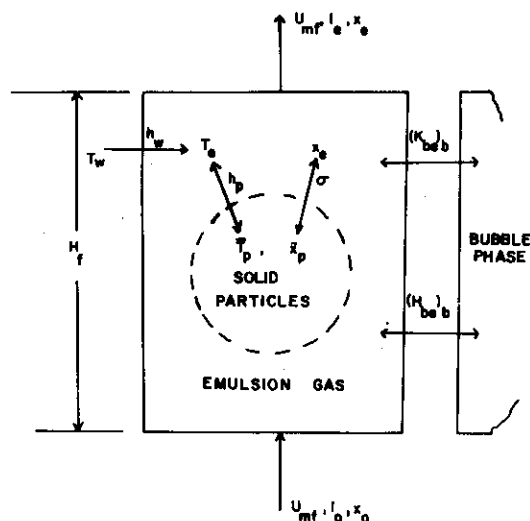


Fig. 2. Mass and energy transfer between solid particles and emulsion gas.

eq. (15) can be rewritten as

$$\rho_s \frac{U_{mf}}{H_f \delta_b} (x_c - x_0) = \rho_g (K_{be})_b (\bar{x}_p - x_c) + \frac{(1 - \epsilon_{mf})(1 - \delta_b)}{\delta_b} \frac{6}{d_p} \sigma (\bar{x}_p^* - x_c) \quad (17)$$

The parameters in the above equation can be evaluated from the following relationships:

1. Evaporation coefficient, σ (Palancz, 1983):

$$\sigma = \frac{h_p \rho_g D_g}{k_g} \quad (18)$$

where

$$h_p = c_g U_0 \rho_g j_h Pr_g^{-2/3} \quad (19)$$

$$j_h = \frac{Nu_p}{Re_p Pr_g^{1/3}} = \begin{cases} 1.77 Re_p^{-0.44} & \text{if } Re_p \geq 30 \\ 570 Re_p^{-0.78} & \text{if } Re_p < 30 \end{cases} \quad (20)$$

with

$$Nu_p = \frac{h_p d_p}{k_g}, \quad Pr_g = \frac{c_g \mu_g}{k_g}, \quad Re_p = \frac{d_p U_0 \rho_g}{(1 - \epsilon_{mf}) \mu_g} \quad (21)$$

2. Average moisture content of the drying gas on the surface of a particle, \bar{x}_p^* :

$$\bar{x}_p^* = \int_0^\infty \frac{1}{t_s} \exp\left(-\frac{t_s}{t_s}\right) x_p^* dt_s \quad (22)$$

where x_p^* may be expressed as (Palancz, 1983)

$$x_p^* = \phi_1(T_p) \phi_2(x_p) \quad (23)$$

with

$$\phi_1(T_p) = 0.622 \frac{P_w}{760 - P_w} \quad (24)$$

and

$$\phi_2(x_p) = \begin{cases} 1 & \text{if } x_p > x_{pc} \\ \frac{x_p^n (x_{pc}^n + K)}{x_{pc}^n (x_p^n + K)} & \text{if } x_p \leq x_{pc} \end{cases} \quad (25)$$

In eq. (24),

$$P_w = 10^{(0.622 + \frac{7.5T_p}{238 + 7p})} \quad (26)$$

and n and K are constants.

(C) *Single solid particle.* A moisture balance around a particle depicted in Fig. 2 results in

$$\rho_s \frac{dx_p}{dt_s} = -\left(1 + \frac{\rho_s}{\rho_w} x_{pc}\right) \frac{6}{d_p} \sigma (x_p^* - x_c) \quad (27a)$$

with the boundary condition

$$x_p = x_{p0} \quad \text{at } t_s = 0. \quad (27b)$$

Equation (27a) is coupled with T_p since x_p^* is a function of both x_p and t_p . The average moisture content of particles, \bar{x}_p , is obtained as

$$\bar{x}_p = \int_0^\infty \frac{1}{t_s} \exp\left(-\frac{t_s}{t_s}\right) x_p dt_s \quad (28)$$

Energy conservation equations

(A) *Bubble phase.* From Fig. 1, a steady-state energy balance around the controlled volume gives

$$\rho_g \frac{U_b}{\delta_b} \frac{di_b}{dz} = (H_{be})_b (T_c - T_b) + \rho_g (K_{be})_b (x_c - x_b) i_{we} \quad (29)$$

where

$$i_b = c_g (T_b - T_{ref}) + x_b [c_{wv} (T_b - T_{ref}) + \gamma_0] \quad (30)$$

$$i_{we} = c_{wv} (T_c - T_{ref}) + \gamma_0 \quad (31)$$

From eq. (3),

$$(K_{be})_b (x_c - x_b) = (K_{be})_b (x_c - x_0) \exp\left(-\frac{(K_{be})_b \delta_b}{U_b} z\right) \quad (32)$$

Using the above three expressions along with eq. (2a), we can rewrite eq. (29) as

$$\frac{dT_b}{dz} = \frac{T_c - T_b}{(c_g + c_{wv} x_b)} \left[\frac{(H_{be})_b \delta_b}{U_b \rho_g} + \frac{\delta_b (K_{be})_b (x_c - x_0) c_{wv}}{U_b} \exp\left(-\frac{(K_{be})_b \delta_b}{U_b} z\right) \right] \quad (33a)$$

The appropriate boundary condition is

$$T_b = T_0 \quad \text{at } z = 0. \quad (33b)$$

$(H_{be})_b$ in eq. (33a) can be determined by (Kunii and Levenspiel, 1969)

$$(H_{be})_b = \frac{1}{1/(H_{be})_b + 1/(H_{ce})_b} \quad (34)$$

where

$$(H_{bc})_b = 4.5 \frac{U_{mf} \rho_g c_g}{d_b} + 5.85 \frac{(k_g \rho_g c_g)^{1/2}}{d_b^{5/4}} g^{1/4} \quad (35)$$

$$(H_{ce})_b = 6.78 (\rho_g c_g k_g)^{1/2} \left(\frac{\varepsilon_{mf} U_b}{d_b^3 \delta_b} \right)^{1/2} \quad (36)$$

(B) *Emulsion gas.* Referring to Fig. 2, a steady-state energy balance around the entire emulsion gas gives

$$\begin{aligned} 0 = & (U_{mf} A_t) \rho_g (i_0 - i_e) + (H_f A_t) (1 - \delta_b) \\ & \times (1 - \varepsilon_{mf}) \frac{6}{d_p} \sigma (\bar{x}_p^* - x_e) \bar{i}_{ws} \\ & + \int_0^{H_f} A_b (H_{bc})_b (T_b - T_c) dz + S_w h_w (T_w - T_c) \\ & - \int_0^{H_f} \rho_g A_b (K_{bc})_b (x_c - x_b) i_{we} dz \\ & - (H_f A_t) (1 - \delta_b) (1 - \varepsilon_{mf}) \frac{6}{d_p} h_p (T_c - \bar{T}_p) \quad (37) \end{aligned}$$

where

$$\bar{i}_{ws} = c_{wv} (\bar{T}_p - T_{ref}) + \gamma_0 \quad (38)$$

$$i_0 = c_g (T_0 - T_{ref}) + x_0 [c_{wv} (T_0 - T_{ref}) + \gamma_0] \quad (39)$$

$$i_e = c_g (T_c - T_{ref}) + x_e [c_{wv} (T_c - T_{ref}) + \gamma_0] \quad (40)$$

$$\bar{T}_p = \int_0^\infty \frac{1}{\bar{t}_s} \exp\left(-\frac{t_s}{\bar{t}_s}\right) T_p dt_s \quad (41)$$

We define the average temperature of gas bubbles, \bar{T}_b , as

$$\bar{T}_b = \frac{1}{H_f} \int_0^{H_f} T_b dz \quad (42)$$

and the specific heat-transfer surface of the dryer wall as

$$a_w = \frac{S_w}{V_{tot}} \quad (43)$$

Insertion of eqs (38)–(43) into eq. (37) yields

$$\begin{aligned} 0 = & \frac{\rho_g U_{mf}}{H_f} \{c_g (T_0 - T_{ref}) + x_0 [c_{wv} (T_0 - T_{ref}) \\ & + \gamma_0] - c_g (T_c - T_{ref}) \\ & - x_e [c_{wv} (T_c - T_{ref}) + \gamma_0]\} + \delta_b (H_{bc})_b (\bar{T}_b - T_c) \\ & + (1 - \delta_b) (1 - \varepsilon_{mf}) \frac{6\sigma}{d_p} (\bar{x}_p^* - x_e) [c_{wv} (\bar{T}_p - T_{ref}) + \gamma_0] \\ & + a_w h_w (T_w - T_c) - (1 - \delta_b) (1 - \varepsilon_{mf}) \frac{6}{d_p} h_p (T_c - \bar{T}_p) \\ & - \rho_g \delta_b (K_{bc})_b (x_c - x_b) [c_{wv} (T_c - T_{ref}) + \gamma_0] \quad (44) \end{aligned}$$

or

$$\begin{aligned} \frac{\rho_g U_{mf}}{H_f} \{c_g (T_c - T_0) + (x_c - x_0) \gamma_0 + c_{wv} [(T_c - T_{ref}) x_c \\ - (T_0 - T_{ref}) x_0]\} = \delta_b (H_{bc})_b (\bar{T}_b - T_c) + (1 - \delta_b) \end{aligned}$$

$$\begin{aligned} & \times (1 - \varepsilon_{mf}) \frac{6}{d_p} \{ \sigma (x_p^* - x_e) [c_{wv} (\bar{T}_p - T_{ref}) + \gamma_0] \\ & - h_p (T_c - \bar{T}_p) \} + \rho_g \delta_b (K_{bc})_b (\bar{x}_b - x_e) \\ & \times [c_{wv} (T_c - T_{ref}) - \gamma_0] + a_w h_w (T_w - T_c) \quad (45) \end{aligned}$$

Eliminating the term $(K_{bc})_b (\bar{x}_b - x_e)$ from the above expression by resorting to eq. (17), eq. (45) can be rewritten as

$$\begin{aligned} & \frac{\rho_g U_{mf}}{H_f} (c_g + c_{wv} x_0) (T_c - T_0) \\ & = \delta_b (H_{bc})_b (\bar{T}_b - T_c) + (1 - \delta_b) (1 - \varepsilon_{mf}) \frac{6}{d_p} (\bar{T}_p - T_c) \\ & \times [c_{wv} \sigma (\bar{x}_p^* - x_e) + h_p] + a_w h_w (T_w - T_c) \quad (46) \end{aligned}$$

The heat-transfer coefficient between air and the dryer wall, h_w , is correlated as (Li and Finlayson, 1977)

$$\frac{h_w d_p}{k_g} = 0.16 Re^{0.93} \quad (47)$$

(C) *Single particle.* Referring to Fig. 3, an unsteady-state energy balance around a particle yields

$$\rho_s \frac{di_p}{dt_s} = \left(1 + \frac{\rho_s}{\rho_w} x_{pc} \right) \frac{6}{d_p} [q_s - \sigma (x_p^* - x_e) i_{ws}] \quad (48)$$

where

$$i_p = c_p (T_p - T_{ref}) + x_p c_w (T_p - T_{ref}) \quad (49)$$

$$i_{ws} = \gamma_0 + c_{wv} (T_p - T_{ref}) \quad (50)$$

The energy balance around the stagnant film surrounding the particle yields (see Fig. 3)

$$q_s + \sigma (x_p^* - x_e) i_{we} = h_p (T_c - T_p) + \sigma (x_p^* - x_e) i_{ws} \quad (51)$$

or

$$q_s - \sigma (x_p^* - x_e) i_{ws} = h_p (T_c - T_p) - \sigma (x_p^* - x_e) i_{we} \quad (52)$$

Insertion of eqs (49), (52) and (31) into eq. (48) and

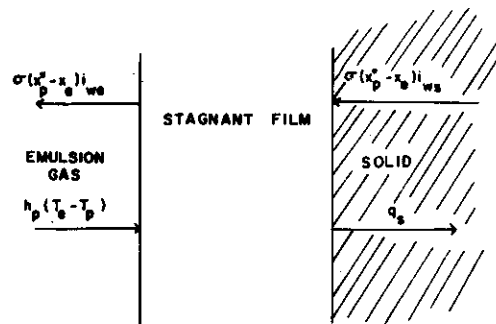


Fig. 3. Energy balance around the stagnant film surrounding a solid particle.

rearrangement of the resultant equation yield

$$\begin{aligned} & \rho_s \left[(c_p + x_p c_w) \frac{dT_p}{dt_s} + c_w (T_p - T_{ref}) \frac{dx_p}{dt_s} \right] \\ &= \left(1 + \frac{\rho_s}{\rho_w} x_{pc} \right) \frac{6}{d_p} \{ h_p (T_c - T_p) - \sigma (x_p^* - x_c) \\ & \quad \times [c_{wv} (T_c - T_{ref}) + \gamma_0] \} \end{aligned} \quad (53)$$

or

$$\begin{aligned} \rho_s (c_p + x_p c_w) \frac{dT_p}{dt_s} &= \left(1 + \frac{\rho_s}{\rho_w} x_{pc} \right) \frac{6}{d_p} \{ h_p (T_c - T_p) \\ & \quad - \sigma (x_p^* - x_c) [c_{wv} (T_c - T_{ref}) + \gamma_0] \} \\ & \quad - \rho_s c_w (T_p - T_{ref}) \frac{dx_p}{dt_s} \end{aligned} \quad (54)$$

Eliminating dx_p/dt_s from eq. (54) by resorting to eq. (27a), we obtain

$$\begin{aligned} \rho_s (c_p + x_p c_w) \frac{dT_p}{dt_s} &= \left(1 + \frac{\rho_s}{\rho_w} x_{pc} \right) \frac{6}{d_p} \{ h_p (T_c - T_p) \\ & \quad - \sigma (x_p^* - x_c) [c_{wv} (T_c - T_{ref}) - c_w (T_p - T_{ref}) + \gamma_0] \} \end{aligned} \quad (55)$$

γ_0 in eq. (54) is to be evaluated at T_{ref} . It can be related to the heat of vaporization at any arbitrary temperature, T , as follows:

$$c_w T_{ref} - c_{wv} T_{ref} + \gamma_0|_{T_{ref}} = c_w T - c_{wv} T + \gamma_0|_T \quad (56)$$

For convenience, we choose $T = 0^\circ\text{C}$. Then,

$$c_w T_{ref} - c_{wv} T_{ref} + \gamma_0|_{T_{ref}} = \gamma_0|_{T=0^\circ\text{C}} \quad (57)$$

Thus, eq. (55) becomes

$$\begin{aligned} & \rho_s (c_p + x_p c_w) \frac{dT_p}{dt_s} \\ &= \left(1 + \frac{\rho_s}{\rho_w} x_{pc} \right) \frac{6}{d_p} [h_p (T_c - T_p) - \sigma (x_p^* - x_c) \\ & \quad \times (c_{wv} T_c - c_w T_p + \gamma_0)] \end{aligned} \quad (58a)$$

with the boundary condition

$$T_p = T_{p0} \quad \text{at} \quad t_s = 0 \quad (58b)$$

and γ_0 to be evaluated at $T = 0^\circ\text{C}$. The average temperature of particles, \bar{T}_p , can be evaluated from

$$\bar{T}_p = \int_0^x \frac{1}{t_s} \exp\left(-\frac{t_s}{t_s}\right) T_p dt_s \quad (59)$$

The moisture content and temperature of the outlet gas, x_{out} and T_{out} , can be evaluated from the moisture and energy balances, respectively:

$$U_0 x_{out} = U_{mf} x_c + U_b x_b (H_f) \quad (60)$$

and

$$\begin{aligned} & U_0 [c_g T_{out} + x_{out} (c_{wv} T_{out} + \gamma_0)] \\ &= U_{mf} [c_g T_c + x_c (c_{wv} T_c + \gamma_0)] \\ & \quad + U_b [c_g T_b (H_f) + x_b (H_f) (c_{wv} T_b (H_f) + \gamma_0)] \end{aligned} \quad (61)$$

Rearrangement gives

$$x_{out} = \frac{1}{U_0} [U_{mf} x_c + U_b x_b (H_f)] \quad (62)$$

and

$$\begin{aligned} T_{out} &= \frac{1}{U_0 (c_g + x_{out} c_{wv})} \{ U_{mf} [c_g T_c + x_c (c_{wv} T_c + \gamma_0)] \\ & \quad + U_b [c_g T_b (H_f) + x_b (H_f) (c_{wv} T_b (H_f) + \gamma_0)] \\ & \quad - U_0 x_{out} \gamma_0 \} \end{aligned} \quad (63)$$

Equations (3), (17), (33a), (46), (27a) and (58a) with the appropriate initial and boundary conditions constitute the governing equations of the present model. To determine the drying characteristics, these equations need be solved simultaneously. Because of the coupling and non-linearity among them, it is necessary to employ numerical solutions.

NUMERICAL SIMULATION

The solution of the model equations is obtained through a two-dimensional trial-and-error procedure. For simplification, first we seek to reduce the integro-differential equations to a set of first-order differential equations. This is achieved by introducing three new intermediate variables.

$$X_p^* = \frac{1}{t_s} \int_0^{t_s} x_p^* \exp\left(-\frac{t_s}{t_s}\right) dt_s \quad (64a)$$

or

$$\frac{dX_p^*}{dt_s} = \frac{x_p^*}{t_s} \exp\left(-\frac{t_s}{t_s}\right) \quad (64b)$$

with the boundary condition

$$X_p^* = 0 \quad \text{at} \quad t_s = 0; \quad (64c)$$

$$T_p^* = \frac{1}{t_s} \int_0^{t_s} T_p \exp\left(-\frac{t_s}{t_s}\right) dt_s \quad (65a)$$

or

$$\frac{dT_p^*}{dt_s} = \frac{T_p}{t_s} \exp\left(-\frac{t_s}{t_s}\right) \quad (65b)$$

with the boundary condition

$$T_p^* = 0 \quad \text{at} \quad t_s = 0; \quad (65c)$$

and

$$T_b^* = \frac{1}{H_f} \int_0^z T_b dz \quad (66a)$$

or

$$\frac{dT_b^*}{dz} = \frac{T_b}{H_f} \quad (66b)$$

with the boundary condition

$$T_b^* = 0 \quad \text{at} \quad z = 0. \quad (66c)$$

Now \bar{x}_p^* , \bar{T}_p and \bar{T}_b can be expressed, respectively, as

$$\bar{x}_p^* = \lim_{t_s \rightarrow \infty} X_p^* \quad (67)$$

$$\bar{T}_p = \lim_{t_s \rightarrow \infty} T_p^* \quad (68)$$

$$\bar{T}_b = T_b^*|_{z=H_f} \quad (69)$$

When t_s exceeds a certain value, e.g. t_s^0 , x_p^* and T_p^* in eqs (64a) and (65a), respectively, remain constant; then, we have

$$\begin{aligned} \bar{x}_p^* &= \frac{1}{t_s} \int_0^\infty x_p^* \exp\left(-\frac{t_s}{t_s}\right) dt_s \\ &= \frac{1}{t_s} \int_0^{t_s^0} x_p^* \exp\left(-\frac{t_s}{t_s}\right) dt_s + \frac{1}{t_s} \int_{t_s^0}^\infty x_p^* \exp\left(-\frac{t_s}{t_s}\right) dt_s \\ &= X_p^*|_{t_s=t_s^0} + x_p^*|_{t_s=t_s^0} \exp\left(-\frac{t_s^0}{t_s}\right). \end{aligned} \quad (70)$$

Similarly,

$$\bar{T}_p = T_p^*|_{t_s=t_s^0} + T_p^*|_{t_s=t_s^0} \exp\left(-\frac{t_s^0}{t_s}\right). \quad (71)$$

Thus, the solution of the governing equations, eqs (3), (17), (33a), (46), (27a) and (58a), can be obtained by solving only a set of first-order differential equations along with several algebraic equations. The calculation procedure is described below.

- (1) Input data.
- (2) Assume the initial values x'_e for x_e and T'_e for T_e .

- (3) Choose t_s^0 , which depends on the speed of convergence and usually is in the range of $1/3\bar{t}_s$ to $2\bar{t}_s$.
- (4) Evaluate

$$X_p^*|_{t_s=t_s^0}, \quad T_p^*|_{t_s=t_s^0} \quad \text{and} \quad T_b^*|_{z=H_f}$$

- through eqs (64b), (65b) and (66b) with the corresponding boundary conditions by using the Runge-Kutta method.
- (5) Calculate \bar{x}_p^* , \bar{T}_p and \bar{T}_b using eqs (70), (71) and (69), respectively.
 - (6) Evaluate x_e and T_e from eqs (17) and (46), respectively.
 - (7) Compare x_e and T_e calculated in step (6) with the initially guessed values x'_e and T'_e . If they are not identical, determine a new pair of initial values of x_e and T_e and repeat steps (1)–(7).
 - (8) Stop when x'_e , T'_e and x_e , T_e are identical.

The stopping criteria used in the present study are

$$|x'_e - x_e| < 10^{-4} \quad \text{and} \quad |T'_e - T_e| < 10^{-2}.$$

For illustration, the following data are considered (Palancz, 1983): $U_0 = 1 \text{ m s}^{-1}$, $T_0 = 250^\circ\text{C}$, $x_0 = 0.015$, $\rho_g = 1 \text{ kg m}^{-3}$, $\rho_s = 2500 \text{ kg m}^{-3}$, $\rho_w = 1000 \text{ kg m}^{-3}$, $\mu_g = 2 \times 10^{-5} \text{ kg m}^{-1} \text{ s}^{-1}$, $k_g = 2.93 \times 10^{-2} \text{ J m}^{-1} \text{ s}^{-1} \text{ }^\circ\text{C}^{-1}$, $c_g = 1.06 \text{ kJ kg}^{-1} \text{ }^\circ\text{C}^{-1}$, $c_p = 1.26 \text{ kJ kg}^{-1} \text{ }^\circ\text{C}^{-1}$, $c_{wv} = 1.93 \text{ kJ kg}^{-1} \text{ }^\circ\text{C}^{-1}$, $c_w = 4.19 \text{ kJ kg}^{-1} \text{ }^\circ\text{C}^{-1}$, $\gamma_0 = 2.5 \times 10^3 \text{ kJ kg}^{-1}$, x_{p0}

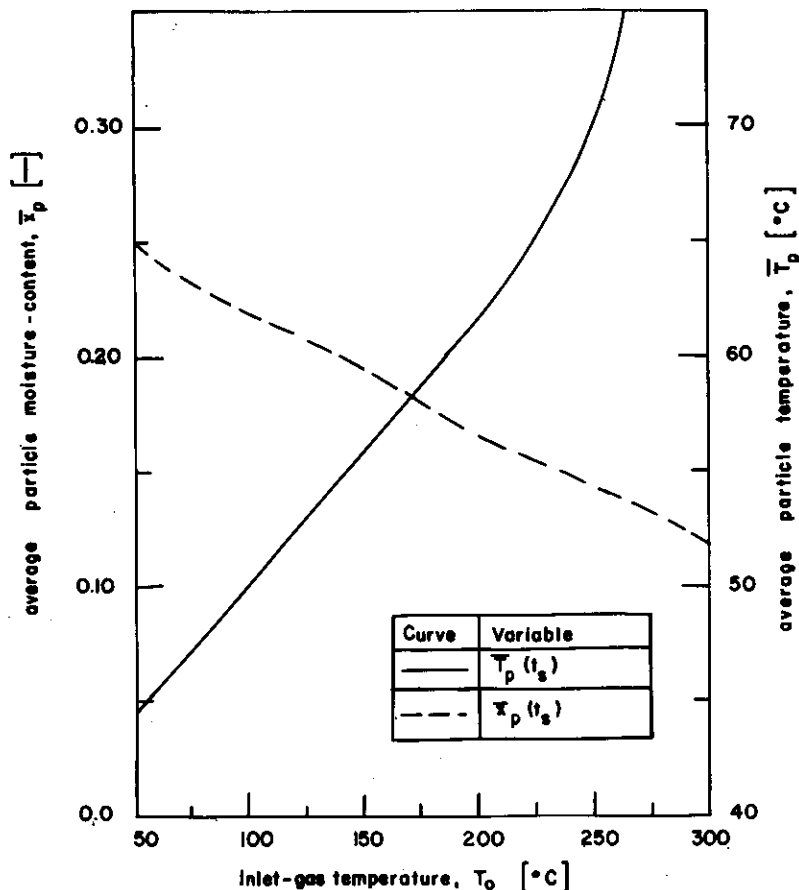


Fig. 4. Effect of the inlet-gas temperature. $T_w = 105^\circ\text{C}$, $T_{p0} = 20^\circ\text{C}$, $U_0 = 1 \text{ m/s}$, $x_{p0} = 0.35$, $x_0 = 0.015$, $t_s = 300 \text{ s}$.

$= 0.35$, $\bar{t}_s = 300$ s, $H_f = 0.5$ m, $D_c = 0.15$ m, $d_b = 2 \times 10^{-2}$ m, $D_g = 2 \times 10^{-5}$ m²s⁻¹, $T_{p0} = 20^\circ\text{C}$, $T_w = 105^\circ\text{C}$, $x_{pc} = 0.2$, $n = 3$, $K = 1 \times 10^{-2}$.

RESULTS AND DISCUSSION

The average moisture content and temperature of particles at the exit are related to the inlet-gas temperature in Fig. 4. Figures 5-7 show the effects of various operating parameters on variations of the temperature and moisture content of a single particle as functions of time. In Fig. 8, the temperature and moisture content of a particle based on Palancz's model are compared with those based on the present model. The three stages of drying can be clearly identified in the $x_p(t_s)$ and $T_p(t_s)$ curves in Figs 5-8. The rather short initial stage of the $T_p(t_s)$ curves, each with a steep positive slope, involves the preheating of a particle, resulting in a sharp rise in its temperature from the inlet value. The subsequent horizontal section represents the constant-rate drying period with the temperature of the particle equal to the wet-bulb temperature. The corresponding portion of the $x_p(t_s)$

curve is a linearly declining section. The remaining portion of each of the two curves represents the falling-rate drying period in which the temperature and moisture content of the particle approach gradually their respective equilibrium values.

Effects of the operating parameters

The performance characteristics of the dryer under various T_0 are revealed in Fig. 4. The higher the temperature of the inlet gas, the higher the temperature of the gas in the bubble and emulsion phases, thus enhancing the rate of evaporation. This, in turn, results in an increase in the average temperature and a decrease in the moisture content of particles at the exit. Note that the T_p curve in Fig. 4 with T_0 less than a certain value (250°C in this example) has a relatively small gradient with respect to T_0 . This implies that the dryer is not highly sensitive to the change in T_0 . To prevent burning or cracking of particles, the drying operation needs to be conducted within this range, where moderate fluctuations in T_0 will not cause overdrying.

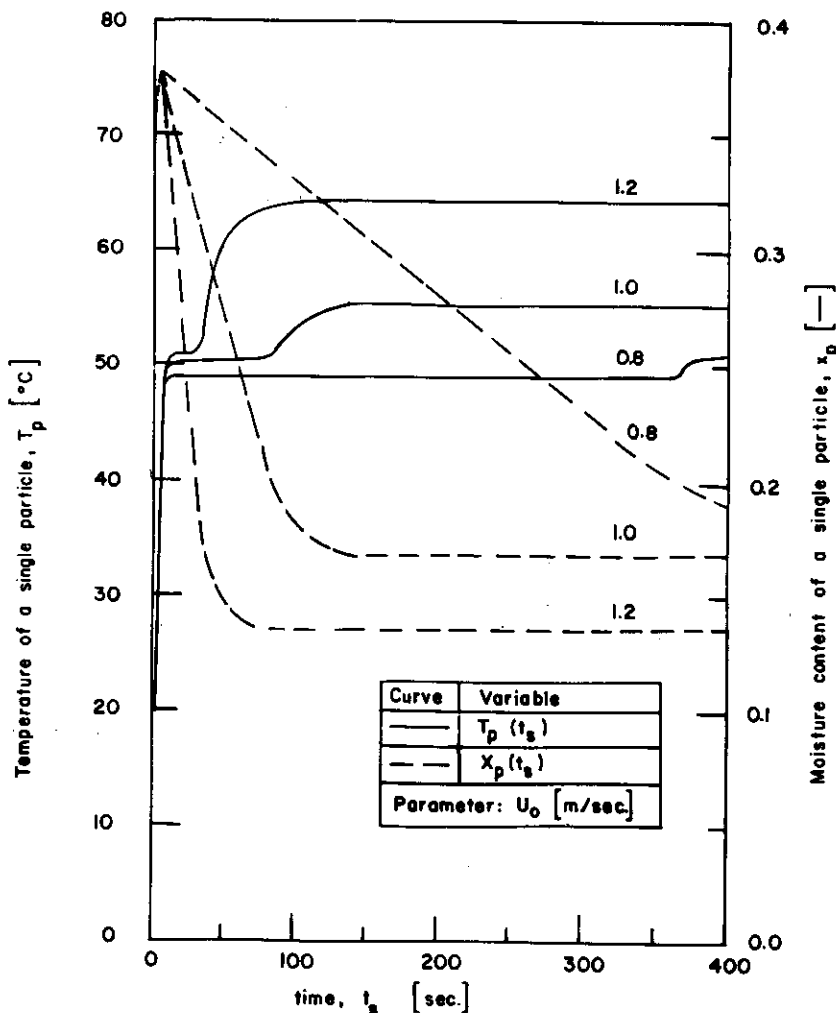


Fig. 5. Effect of the superficial gas velocity. $T_0 = 250^\circ\text{C}$, $T_{p0} = 20^\circ\text{C}$, $T_w = 50^\circ\text{C}$, $x_{p0} = 0.35$, $x_0 = 0.015$, $\bar{t}_s = 300$ s.

The influence of the superficial gas velocity on the performance characteristics of the dryer can be discerned in Fig. 5. When U_0 increases, the average temperature of particles at the exit increases appreciably while their average moisture content reduces sharply. This can be attributed to the intensified mass and heat transfer among bubbles, emulsion gas and solids. Figure 5 shows that the gradients of the $T_p(t_s)$ and $x_p(t_s)$ curves are substantially increased in the constant-rate drying period. It is worth noting that these gradients are not affected as significantly by the change in U_0 in the falling-rate period as they are in the constant-rate drying period. This phenomenon suggests that the fluidized-bed dryer is effective in enhancing the drying rate mainly in the constant-rate drying period. The relationship between the superficial gas velocity and the length of the constant-rate drying period can be roughly approximated by the expression

$$t_s = 4.8 \times 10^4 e^{-6.2U_0}$$

which should be of practical use in the design of the fluidized-bed dryer.

The effect of the dryer-wall temperature on the variations of the moisture content and temperature of an individual particle as functions of time can be observed in Fig. 6. Naturally, a rise of wall temperature increases the rate of heat transfer to the emulsion gas. This leads to an increase in temperature of the emulsion gas, thereby enlarging the driving force for evaporation of moisture from the particle. Consequently, the average temperature of particles at the exit increases while their average moisture content decreases.

The effect of the mean residence time of particles on the dryer performance is illustrated in Fig. 7. With the bed height fixed, the smaller the mean residence time, the larger the feed flow rate of solids and the shorter the contact time between the particles and drying gas. This results in a relatively low average temperature and a high moisture content for the particles at the exit.

Comparison with an existing mechanistic model

A mechanistic model proposed by Palancz (1983) gives a comprehensive description of the heat and mass

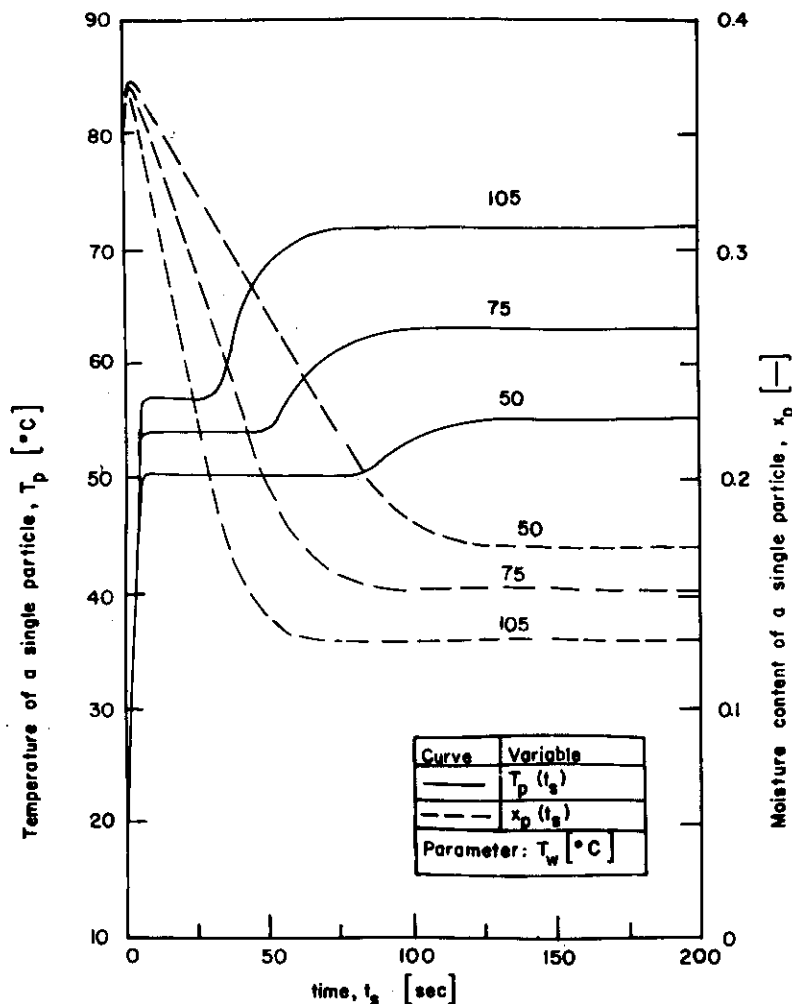


Fig. 6. Effect of the dryer-wall temperature. $T_0 = 250^\circ\text{C}$, $T_{p0} = 20^\circ\text{C}$, $U_0 = 1 \text{ m/s}$, $x_{p0} = 0.35$, $x_0 = 0.015$, $\bar{t}_s = 300 \text{ s}$.

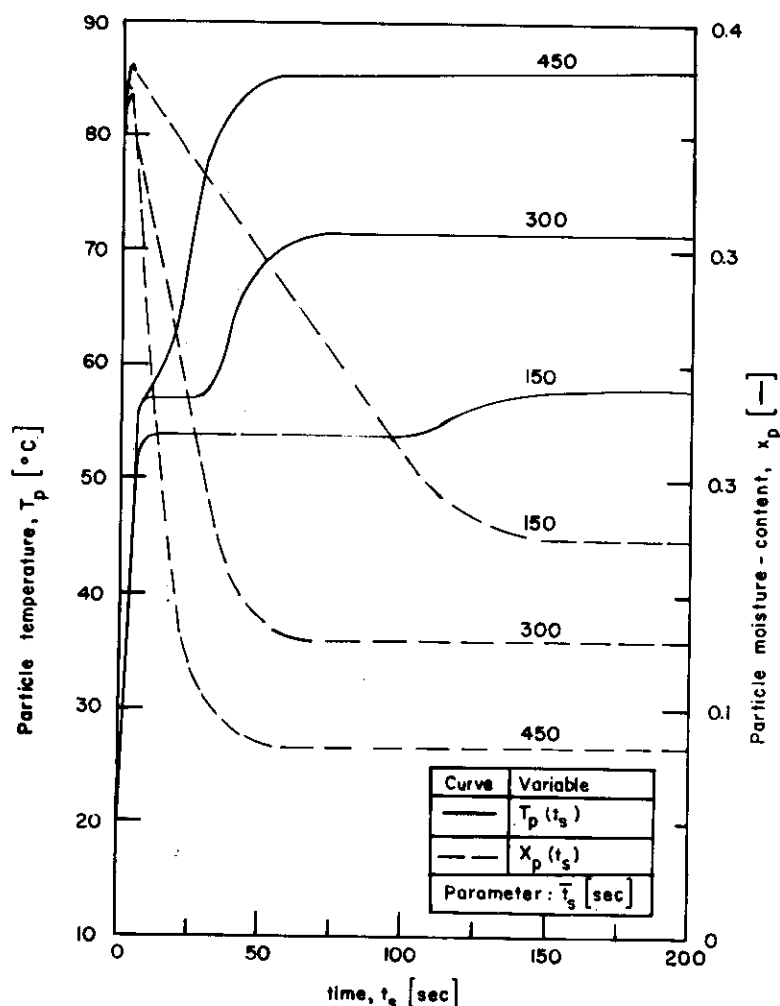


Fig. 7. Effect of the mean residence time of particles. $T_0 = 250^\circ\text{C}$, $T_w = 105^\circ\text{C}$, $T_{p0} = 20^\circ\text{C}$, $U_0 = 1 \text{ m/s}$, $x_{p0} = 0.35$, $x_0 = 0.015$.

transfer among gaseous and solid phases in a continuous fluidized-bed dryer. It is free of the assumptions that the drying gas is homogeneous and that exit streams are in equilibrium. Palancz's model appears to be the only existing model comparable to the present one. In fact, the present model is an exhaustive amendment and a substantial extension of Palancz's model. The major differences between the two models are as follows:

1. To simplify the governing equations of his model and to facilitate its solution, Palancz has imposed an assumption that the specific heat of the drying gas remains constant throughout the entire drying process. In other words,

$$c_g = x_e c_{wv} = \text{constant}$$

and

$$c_g = x_b c_{wv} = \text{constant.}$$

The second expression implies that the moisture content of gas bubbles, x_b , remains constant, which is contradictory to the plug flow postulate for the bubble phase. Moreover, when moisture evaporates into the

drying gas from solids, an appreciable amount of moisture migrates from the emulsion gas to the bubbles; it is not plausible that its accompanying thermal energy can be neglected. A consequence of this assumption is that in Palancz's model, the energy conservation equation for the bubble phase, which corresponds to eq. (33a), is linear and only contains the first term on the right-hand side of the equation. Subsequently, in his energy conservation equation for the emulsion gas, the term designating the energy transfer accompanied by the evaporation of moisture contains only T_e instead of $T_p - T_e$. This means that the energy conservation equation depends on the choice of reference temperature, which is impossible.

2. To evaluate the equilibrium moisture content of the drying gas on the surface of a particle, Palancz's model resorts to the approximate expression

$$x_p^* = \phi_1(T_p)\phi_2(x_p)$$

with

$$\phi_1(T_p) = 0.622 \frac{P_{w'}}{760 - P_w}$$

and

$$\phi_2(x_p) = \begin{cases} 1 & \text{if } x_p > x_c \\ \frac{x_p^n}{x_p^n(x_p^n + K)} & \text{if } x_p \leq x_c. \end{cases}$$

Note that a discontinuity occurs at $x_p = x_{pc}$ in the expression for $\phi_2(x_p)$; this is illogical. In contrast, the corresponding expression of the present model, eq. (23), does not contain such a discontinuity.

The $x_p(t_s)$ and $T_p(t_s)$ curves of the present model are compared with those of Palancz's model in Fig. 8. The values of $T_p(t_s)$ and $x_p(t_s)$ of the latter obviously are much higher than those of the former. As mentioned earlier, the latter neglects the net outflow of moisture from the emulsion phase to the bubble phase and its accompanying thermal energy transfer. This is tantamount to including extra mass and thermal energy in the emulsion gas in establishing mass and energy balances around it. As a result, relatively high values of x_c and T_c are expected, which in turn lead to an overestimation of the values of \bar{x}_p and \bar{T}_p .

CONCLUSION

A fairly rigorous mechanistic model is presented for a continuous fluidized-bed dryer. The influences of the various operating parameters have been investigated. The results of numerical simulation indicate that the performance characteristics of the dryer are affected significantly by the superficial gas velocity, the inlet temperature of the drying gas, the mean residence time of solids and the dryer-wall temperature. These results also indicate that the fluidized-bed dryer is effective in enhancing the drying rate mainly in the constant drying period. Thus, it appears advisable that a fluidized-bed dryer be used in series with a conventional moving-bed or packed-bed dryer; the latter serves to dry particles with bound moisture content.

In drying, the moisture content of the drying gas is appreciably increased by evaporation of moisture from solids. As a result, there is a substantial energy transfer to the drying gas accompanied by moisture migration. The present model incorporates the change in the specific heat of the drying gas due to this moisture migration. This is in contrast to the model proposed by

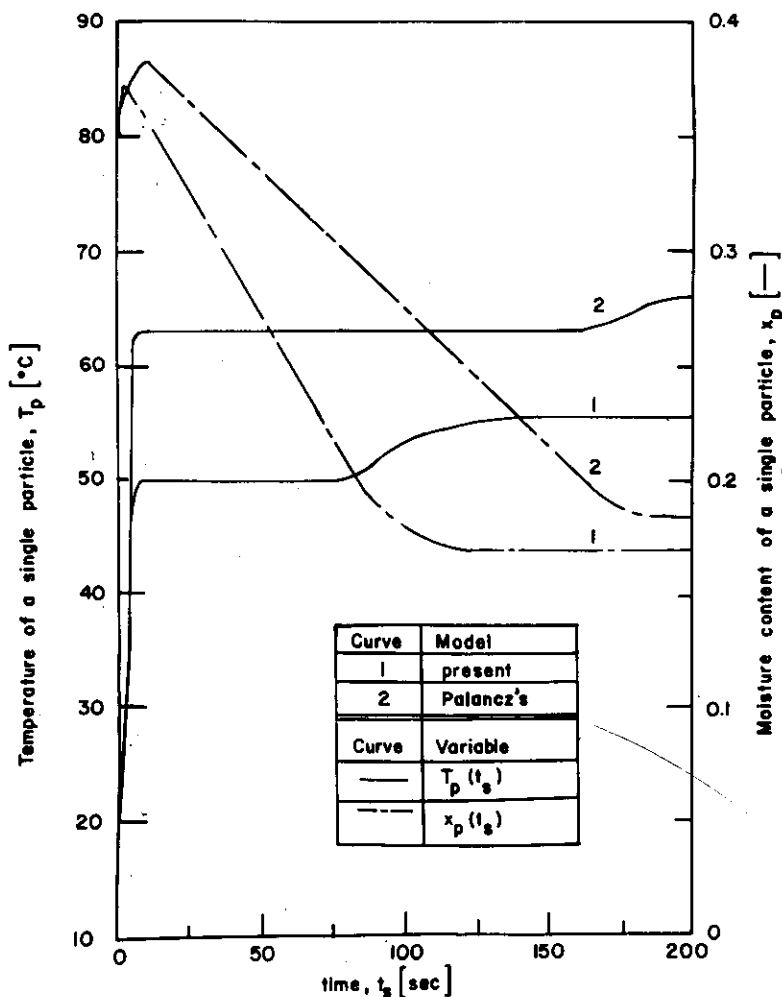


Fig. 8. Comparison of the present model with Palancz's model. $T_0 = 250^\circ\text{C}$, $T_w = 50^\circ\text{C}$, $T_{p0} = 20^\circ\text{C}$, $U_0 = 1 \text{ m/s}$, $x_{p0} = 0.35$, $x_0 = 0.015$, $\bar{t}_s = 300 \text{ s}$.

Palancz, which assumes a constant specific heat for the drying gas. The results of simulation have proved that this assumption leads to an overestimation of the temperature and moisture content of particles.

It is unlikely that the moisture content of the drying gas on the surface of a particle can undergo a discontinuity as suggested in Palancz's model. The present model does not contain such a discontinuity, and thus should be more rational in expressing heat and mass-transfer relationships between the drying gas and solids.

NOTATION

A_t	cross-sectional area of the bed, m^2	$(K_{bc})_b$	bubble and cloud-wake regions based on the volume of bubbles, s^{-1}
A_b	cross-sectional area of the bubble phase, m^2	$(K_{ce})_b$	coefficient of gas interchange between the bubble and emulsion phases based on the volume of bubbles, s^{-1}
a_w	specific heat-transfer surface of the dryer wall, m^{-1}	k_g	coefficient of gas interchange between the cloud-wake region and the emulsion phase based on the volume of bubbles, s^{-1}
c_g	specific heat of drying gas, $kJ kg^{-1} ^\circ C^{-1}$	Le	thermal conductivity of the drying gas, $J m^{-1} ^\circ C^{-1}$
c_p	specific heat of particles (dry basis), $kJ kg^{-1} ^\circ C^{-1}$	Le	Lewis number, dimensionless
c_w	specific heat of water (liquid state), $kJ kg^{-1} ^\circ C^{-1}$	Nu	Nusselt number, dimensionless
c_{wv}	specific heat of water vapour, $kJ kg^{-1} ^\circ C^{-1}$	Pr	Prandtl number, dimensionless
D_c	diameter of the bed column, m	P_w	pressure of saturated water vapour, mm Hg
D_g	molecular diffusion coefficient of the drying gas, $m^2 s^{-1}$	q_s	conductive heat flux inside a particle, $J s^{-1} m^{-2}$
D_{eff}	effective diffusion coefficient of the drying gas, $m^2 s^{-1}$	Re_p	particle Reynolds number, dimensionless
d_b	effective bubble diameter, m	S_w	heat-transfer surface area of the dryer wall, m^2
d_p	particle diameter, m	T_0	temperature of the inlet gas, $^\circ C$
g	gravitational acceleration, $m s^{-2}$	T_b	temperature of gas bubbles, $^\circ C$
H_f	expanded bed height, m	\bar{T}_b	bed-height average temperature of gas bubbles, $^\circ C$
H_{mf}	bed height at minimum fluidizing conditions, m	T_c	temperature of the emulsion gas, $^\circ C$
$(H_{bc})_b$	volumetric heat-transfer coefficient between the bubble and cloud-wake regions based on the volume of bubbles, $J s^{-1} m^{-3} ^\circ C^{-1}$	T_{out}	temperature of the outlet gas
$(H_{be})_b$	volumetric heat-transfer coefficient between the bubble and emulsion phases based on the volume of bubbles, $J s^{-1} m^{-3} ^\circ C^{-1}$	T_p	temperature of a particle, $^\circ C$
$(H_{ce})_b$	volumetric heat-transfer coefficient between the cloud-wake region and the emulsion phase based on the volume of bubbles, $J s^{-1} m^{-3} ^\circ C^{-1}$	\bar{T}_p	average temperature of particles, $^\circ C$
h_p	heat-transfer coefficient between the drying gas and solids, $J s^{-1} m^{-2} ^\circ C^{-1}$	T_{p0}	temperature of inlet particles, $^\circ C$
h_w	heat-transfer coefficient between the drying gas and the dryer wall, $J s^{-1} m^{-2} ^\circ C^{-1}$	T_{ref}	reference-state temperature, $^\circ C$
i_0	enthalpy of inlet gas (dry basis), $kJ kg^{-1}$	T_w	dryer-wall temperature, $^\circ C$
i_b	enthalpy of gas bubbles (dry basis), $kJ kg^{-1}$	t_s	time, s
i_c	enthalpy of the emulsion gas (dry basis), $kJ kg^{-1}$	\bar{t}_s	mean residence time of particles in the dryer, s
i_{ws}	enthalpy of water vapour on the surface of a particle, $kJ kg^{-1}$	U_0	superficial gas velocity (measured on an empty bed basis) through a bed of solids, $m s^{-1}$
\bar{i}_{ws}	average enthalpy of water vapour on the surface of particles, $kJ kg^{-1}$	U_b	superficial gas velocity in the bubble phase, based on total cross-sectional area of the bed, $m s^{-1}$
i_{wc}	enthalpy of water vapour contained in the emulsion gas, $kJ kg^{-1}$	U_{br}	linear velocity of a single bubble, $m s^{-1}$
i_p	enthalpy of a particle (wet basis), $kJ kg^{-1}$	U_{mf}	superficial gas velocity at minimum fluidizing conditions, $m s^{-1}$
j_p	Colburn factor	V_t	volume of the bed, m^3
$(K_{bc})_b$	coefficient of gas interchange between the	x_0	moisture content of inlet gas (dry basis), dimensionless
		x_b	moisture content of gas bubbles (dry basis), dimensionless
		\bar{x}_b	bed-height average moisture content of gas bubbles (dry basis), dimensionless
		x_c	moisture content of the emulsion gas (dry basis), dimensionless
		x_{out}	moisture content of outlet gas (dry basis), dimensionless
		x_p	moisture content of a particle (dry basis), dimensionless
		\bar{x}_p	average moisture content of particles (dry basis), dimensionless
		x_p^*	moisture content of the drying gas on the surface of a particle (dry basis), dimensionless
		\bar{x}_p^*	average moisture content of the drying gas

	on the surface of a particle (dry basis), dimensionless
x_{p0}	moisture content of inlet particles (dry basis), dimensionless
x_{pc}	critical moisture content of a particle (dry basis), dimensionless
z	elevation, m

Greek letters

γ_0	heat of vaporization, kJ kg^{-1}
δ_b	fraction of the fluidized bed consisting of bubbles, dimensionless
ε_c	void fraction in the emulsion phase, dimensionless
ε_{mf}	void fraction at minimum fluidizing conditions, dimensionless
μ_g	viscosity of gas, $\text{kg m}^{-1} \text{s}^{-1}$
ρ_g	density of gas, kg m^{-3}
ρ_s	density of dry solids, kg m^{-3}
ρ_w	density of water, kg m^{-3}
ρ_{ws}	density of wet solids, kg m^{-3}
σ	evaporation coefficient, $\text{kg m}^{-2} \text{s}^{-1}$
ϕ_s	sphericity of a particle, dimensionless

REFERENCES

- Babu, S. P., Shah, B. and Talwalkar, A., 1978, Fluidization correlation for coal gasification materials—minimum fluidization velocity and fluidized bed expansion ratio. *A.I.Ch.E. Symp. Ser.* 74, 176–186.
- Broadhurst, T. E and Becker, H. A., 1975, Onset of fluidization and slugging in beds of uniform particles. *A.I.Ch.E. J.* 21, 238–247.
- Davison, J. F. and Harrison, D., 1963, *Fluidized Particles*, Chap. 1, pp. 19–20. Cambridge University Press, Cambridge.
- Kato, K., Omura, S., Taneda, D., Onozania, I. and Iijima, A., 1981, Drying characteristics in a packed fluidized bed dryer. *J. chem. Engng Jap.* 14, 365–371.
- Kunii, D. and Levenspiel, O., 1969, *Fluidization Engineering*, Chap. 7, Wiley, New York.
- Li, C. H. and Finlayson, B. A., 1977, Heat transfer in packed beds—a reevaluation. *Chem. Engng Sci.* 38, 147–153.
- Nonhebel, G. and Moss, A. A. H., 1971, *Drying of Solids in the Chemical Industry*, Chap. 11. Butterworth, London.
- Palancz, B., 1983, A mathematical model for continuous fluidized bed drying. *Chem. Engng Sci.* 38, 1045–1059.
- Palancz, B. and Parti, M., 1973, Examination of the heat-and-moisture-content variations in granular bed types. *Acta Tech. Acad. Sci. Hung.* 74, 441–461.
- Vaněček, V., Markvart, M. and Drbohlav, R., 1966, *Fluidized Bed Drying* (Translated by Landau, J.). Leonard Hill, London.
- Viswanathan, K., Subba Rao, D. and Raychaudhury, B. C., 1982, Coherent representation of the drying of gas and solids in fluidized beds. *Ind. chem. Engng* 14, 12–23.
- Wen, C. Y. and Yu, Y. H., 1966, A generalized method for predicting the minimum fluidization velocity. *A.I.Ch.E. J.* 12, 610–612.

Babu, S. P., Shah, B. and Talwalkar, A., 1978, Fluidization correlation for coal gasification materials—minimum